



# Heavy metal pollution in the soil of a riverine basin: distribution, source, and potential hazards

Kifayatullah Khan · Abdul Mohsin · Hafiz Muhammad Adeel Sharif · Afsheen Maryam · Jafar Ali · Xu Li · Sobhy Mostafa Ibrahim · Muhammad Ayaz · Yunqiao Zhou · Muhammad Younas

Received: 24 March 2022 / Accepted: 11 July 2022 / Published online: 29 July 2022  
© The Author(s), under exclusive licence to Springer Nature Switzerland AG 2022

**Abstract** Soil pollution with heavy metals (HMs) has become a world environmental problem. This study focuses on surface soil contamination with Cr, Mn, Co, Ni, Cu, Zn, Cd, Hg, Pb, Fe, and Al, their sources, and potential hazards along the basin of River Swat, Pakistan. The average concentrations (mg/kg) of HMs were the most abundant for Al (24,730.19) followed by Fe (22,419.41) > Mn (386.78) > Zn (57.75) > Cr (38.07) > Ni (32.46) > Cu (23.43) > Pb

(19.59) > Co (10.77) > Cd (3.18) > Hg (0.12). The concentrations of Cr and Mn in 5.45% each, Co in 10.90%, Zn in 27.27%, Cu in 36.36%, Ni in 41.81%, and Hg in 92.72% of the total soil samples exceeded their respective background values. The geostatistical approaches determined the distribution patterns of HM pollution along the basin, whereas the statistics of principal component analysis exposed the likely sources of HM contamination in the area. Pollution indices evaluated

## Highlights

- Geospatial distribution of heavy metals in surface soil was identified.
- Soil contamination was assessed using various pollution indices.
- Potential sources of heavy metals were discerned using multivariate statistics.
- Ecological hazard of heavy metals in soil system was determined using *PEHI* model.
- Heavy metal toxicity to humans was evaluated using potential soil exposed routes.

**Supplementary Information** The online version contains supplementary material available at <https://doi.org/10.1007/s10661-022-10287-2>.

K. Khan (✉) · Y. Zhou  
State Key Laboratory of Urban and Regional Ecology,  
Research Center for Eco-Environmental Sciences, Chinese  
Academy of Sciences, Beijing 100085, China  
e-mail: drkhan@uswat.edu.pk

K. Khan · A. Mohsin · M. Ayaz · M. Younas  
Department of Environmental and Conservation Sciences,  
University of Swat, Swat, 19130, Pakistan

H. M. A. Sharif  
Research Center for Eco-Environmental Engineering,  
Dongguan University of Technology, Dongguan 523808,  
China

A. Maryam  
Department of Environmental Science -ACES-B  
(Institutionen För Miljövetenskap), Stockholm University,  
Stockholm 106 91, Sweden

J. Ali  
Jilin Provincial Key Laboratory of Water Resources  
and Environment, Jilin University, Changchun 130021,  
China

X. Li  
Institute of Quality Standard and Testing Technology,  
Beijing Academy of Agriculture and Forestry Sciences,  
Beijing 100097, China

S. M. Ibrahim  
Department of Biochemistry, College of Science,  
King Saud University, P.O. Box: 2455, Riyadh 11451,  
Saudi Arabia

the overall HM distribution and pollution status in the area. Contamination factor showed a high degree of HM contamination in 82% of the total sampling sites, while the geo-accumulation index designated low to moderate contamination with Cr, Mn, Co, Ni, Cu, Zn, Hg, and Pb, and moderate to extreme contamination with Cd, Fe, and Al. The trend of ecological toxicity showed potential ups and downs along with the sites from low to considerable hazard ( $<95 < PEHI < 190$ ), whereas the human carcinogenic hazard was within the USEPA acceptable limits ( $1 \times 10^{-7} - 1 \times 10^{-4}$ ), but the non-carcinogenic hazard was higher than the threshold ( $HI > 1$ ) for children because they are more exposed than adults.

**Keywords** Heavy metals · Spatial distribution · Multivariate statistics · Pollution indices · Source apportionment · Environmental hazards

## Introduction

By definition, heavy metals (HMs) are those elements having an atomic number greater than 20 and atomic density above  $5 \text{ g cm}^{-3}$  and must exhibit the properties of metal (Raychaudhuri et al., 2021). In recent era, the environmental contamination of HMs has received much global attention because of their high bioaccumulation, toxicity, and tenacity in nature (Chen et al., 2018; Liu et al., 2017; Singh & Kumar, 2017). HMs such as chromium (Cr), manganese (Mn), cobalt (Co), nickel (Ni), copper (Cu), zinc (Zn), cadmium (Cd), mercury (Hg), lead (Pb), iron (Fe), and aluminum (Al) and related compounds are abundant in the environment (Gu et al., 2014; Hu & Cheng, 2013; Jia et al., 2018; Stafilov et al., 2010; ur Rehman et al., 2018). Aside from natural processes, excessive enrichment of HM inaccessible environmental matrices and ecology has resulted in fast urbanization, expanding industries, traffic emissions, and agricultural and mining activities in the past several decades (Iqbal et al., 2016; Kang et al., 2017). Among the environmental matrices, soil acts as a possible sink and a significant transmission source for numerous pollutants, including HMs, into the air, water, and other life-supporting systems (Facchinelli et al., 2001). Excessive application of chemical products, particularly those used for crop growth, is a major pathway for elevated HM concentration in agricultural soil, which has flashed growing

academic and public concerns around the world due to its negative effects on food safety and human health through dermal contact, inhalation, and ingestion of contaminated food chains (Cai et al., 2015; Liu et al., 2017; Qiutong & Mingkui, 2017).

Among the HMs, Zn, Cu, Ni, Mn, Cr, and Fe are fundamentally needed in many structural and biochemical activities in plants and animals, including growth, oxidation–reduction reactions, electron transport, and many other metabolic processes (Kabata-Pendias, 2000). Zn deficiency can induce anorexia, dermatitis, depression, poor wound healing, diarrhea as well as dysfunction of the immune system; however, its poisoning can cause sideroblastic anemia as well (Muhammad et al., 2011). Co, Pb, Cd, and Hg are carcinogenic where its chronic exposure might cause unknown biological functions even at low concentration it may result in cancer along with dermal lesions, anemia, neurotoxicity, lung damage, peripheral neuropathy, and peripheral vascular disease (Sani et al., 2017; Shahid et al., 2017). That is why, the World Health Organization (WHO), the United States Environmental Protection Agency (USEPA), and other regulatory bodies from across the world have designated HMs as priority control pollutants, with maximum health-based guidelines for their contamination in surface soil (Khan et al., 2010; Rodrigues et al., 2013).

In recent decades, surveys on HM contamination related to aquatic rivers, bays and coasts, non-urban mines industrial, transportation, residential areas, and crops have been conducted worldwide. However, the contamination status of HMs in the surface soil is very unknown and needs to be estimated on priority (Bing et al., 2016; Chen et al., 2012, 2015; Li et al., 2014; Pan et al., 2017; Sun et al., 2010). Globally limited studies have been conducted on urban and agricultural soil HM contamination and potential hazards using various pollution evaluation index analyses (Islam et al., 2015; Tian et al., 2016; Wu et al., 2018). However, no studies on pollution levels and health hazards of soil HMs in the Swat River basin, Pakistan, have been conducted yet, indicating a knowledge vacuum in comprehending the possible consequences of soil HMs on human health and ecology. Therefore, to better understand the potential hazards of surface soil with HM contamination in the region, this study aimed to investigate the level of HM pollution and evaluate their possible toxicity along the Swat River

basin (Fig. 1) using multiple pollution evaluation indices as well as the USEPA developed non-carcinogenic and carcinogenic hazard assessment models.

### Materials and methods

#### Study area description

This research was conducted along with the basin soil of River Swat, Khyber Pakhtunkhwa, Pakistan (Fig. 1). River Swat is a tributary river of River Kabul, created by the confluence of the Gabriel and Ushu rivers near Kalam, then flows southerly, then westward till it meets the River Panjkora (Khan et al., 2013b). After a 320-km journey, the combined river enters the Peshawar Plain and meets the Kabul River near Nisatta. It irrigates around 160,000 acres of sugarcane, wheat, and vegetable crops in the districts of Swat, Malakand, and lower Peshawar Valley, as well as feeding the nearby groundwater aquifers (Khan et al., 2022). The total river’s catchment/basin of this river is approximately 13,000 km<sup>2</sup>, which geographically stretched between 34° 06' 60.00" N latitude and 71° 42' 59.99" E longitude. Geologically, the bare rocks in the basin are made of mafic and ultramafic rock materials such as serpentinite, greenschist, talc-carbonate schist, and met basalts, with a sandy loam soil with a maximum land slop of

22% and a depth of 0–45 cm (Khan et al., 2013a, b, 2014, 2022). The contamination of HMs in the basin’s surface soil has been greatly influenced throughout time by anthropogenic inputs such as industrial discharge, agrofertilizers, and commercial and household sewages, all of which discharged dangerous chemicals into the surrounding environment.

#### Soil sampling and pre-treatment

Sampling surveys were designed to randomly collect surface soil samples ( $n=55$ ) from a 20 by 10 cm (deep/width) borehole dug with a stainless-steel auger across the Swat River basin in Khyber Pakhtunkhwa, Pakistan, using a global positioning system (GPS) (Fig. 1). Each soil sample was collected by taking five sub-samples at random distances of about 10 m in various directions surrounding each sampling point, then thoroughly mixing them together using the quartile approach to form a composite sample of 1 kg in a polyethylene bag (Wu et al., 2010). Thereafter, all the collected soil samples were properly transported to the laboratory in an icebox, where they were first homogenized and then air-dried for a few days at ambient temperature before being passed through a sieve with a mesh size of up to 2 mm and stored in high-density polyethylene (HDPE) bags at  $4 \pm 2$  °C for onward chemical analysis.

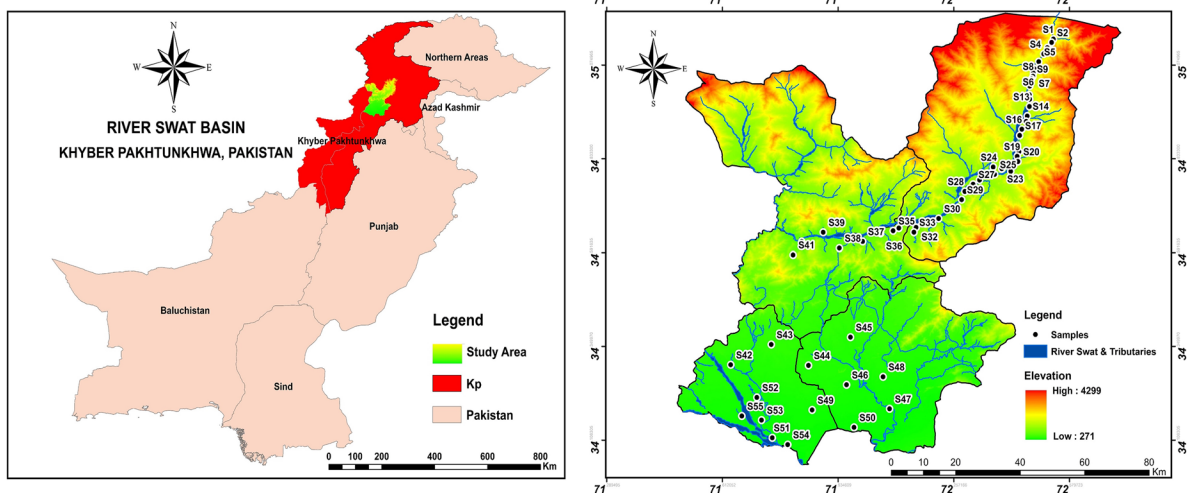


**Fig. 1** The study area’s location map shows sample sites around the River’s Swat basin in Khyber Pakhtunkhwa, Pakistan

## Sample extraction

At the State Key Laboratory of Urban and Regional Ecology, Research Center for Eco-Environmental Sciences, Chinese Academy of Sciences, Beijing, China, all the pre-treated soil samples (0.5 g each) were acid digested in a 5:1:1 ratio of  $\text{HNO}_3$ ,  $\text{H}_2\text{SO}_4$ , and  $\text{HClO}_4$ , respectively, as described in existing literature (Agomuo & Amadi, 2017; Khan et al., 2013a; Nawab et al., 2015; Zheng et al., 2020). After that, all the acid mixed samples were kept overnight for cold digestion before being slowly heated on a hot plate at 80 °C until a transparent extract was formed. Finally, each sample extract was filtered (0.45 m) into a clean polypropylene (PP) tube, and diluted to a level of 50 mL with highly purified Milli-Q water, before stored at room temperature for onward spectrometry analysis.

## Heavy metal's determination and quality control

The concentrations of Cr, Mn, Co, Ni, Cu, Zn, As, Cd, Hg, and Pb in the extracted surface soil samples were determined using inductively coupled plasma-mass spectrometry (ICP-MS, ELANDRC-e, PerkinElmer SCIEX, USA), whereas Fe and Al were examined using inductively coupled plasma optical emission spectrometry (ICP-OES, PerkinElmer SCIEX, USA; ICP-OES, Optima 8000, PerkinElmer, USA). During the analysis, all the quality assurance (QA) and quality control (QC) measures were thoroughly validated. Sample duplicates, field, transport, process, and solvent blanks were collected/prepared continually with each lot of samples to ensure the accurateness of sampling, extraction, and analytical procedures. All essential analytical grade reagents were made in ultrapure Milli-Q water, while standard solutions of the targeted HMs were created by diluting their corresponding 1000 mg/L certified solutions (Khan et al., 2013a, 2022). The accuracy and precision of the ICP-MS and ICP-OES analyses were continuously checked using reagent blanks, duplicates, and certified reference GBW07425-GSS-11 materials provided by the National Research Center for Certified Reference Materials, Beijing, China. All the instrumental analyses were carried out in replicate with a  $\pm 5\%$  relative standard deviation (RSD) to ensure a satisfactory agreement between the concentrations of examined HMs and quality control samples, with certified

reference material percentage recoveries ranging from 87 to 113% (Table S1).

## Evaluation methods of heavy metal pollution

Pollution index analyses, such as contaminator factor ( $CF$ ), degree of contamination ( $CD$ ), geo-accumulation index ( $I_{geo}$ ), and enrichment factor ( $EF$ ), were practiced in the study to evaluate the degree of HM pollution in the soil environment.

### Contamination factor

The  $CF$  of HMs calculated by Eq. (1) is the ratio of Cr, Mn, Co, Ni, Cu, Zn, Cd, Hg, Pb, Fe, and Al concentrations ( $C_n$ ) in surface soil to their background value ( $B_v$ ) of 80, 615, 15, 32, 26, 80, 0.11, 0.06, 32, 38.9, and 78.1 mg/kg, respectively (Jia et al., 2018). As per previous literature (Hakanson, 1980), the  $CF$  values less than one ( $CF < 1$ ) suggest low contamination, the  $CF$  values between  $1 < CF < 3$  indicate moderate contamination, the  $CF$  values between  $3 < CF < 6$  designate considerable contamination, while the  $CF$  values more than 6 ( $CF > 6$ ) signify very high contamination level in the area.

$$CF = \frac{C_n}{B_v} \quad (1)$$

### Degree of contamination

To simplify the control of HM pollution, Hakanson (1980) developed a tool termed the “ $CD$ ” which could be calculated using Eq. (2) as a sum of each metal's  $CF$ s. The recommended classifications for contamination degree that indicate the concerning anthropogenic pollution in the area are the  $CD$  values less than 6 ( $CD < 6$ ), between  $(6 < CD < 12)$ , between  $(12 < CD < 24)$ , and more than 24 ( $CD > 24$ ), representing the low, moderate, considerable, and high degree of contamination, respectively.

$$CD = \sum_i^n CF \quad (2)$$

### Geo-accumulation index

The  $I_{geo}$  model (Eq. (3)) proposed by Muller (1979) was utilized in this study to quantify the overall

possible hazard of each studied HM resulting from the surrounding anthropogenic activities (Sungur & Özcan, 2015).

$$I_{geo} = \log_2 \left[ \frac{C_n}{1.5 \times B_n} \right] \tag{3}$$

where  $C_n$  is the studied HM concentration (mg kg<sup>-1</sup>) in soil,  $B_n$  is the background contamination value (mg kg<sup>-1</sup>) of a given metal (Jia et al., 2018), and coefficient of 1.5 is the contact factor used to assess natural variations of HMs and to detect minor anthropogenic impacts. The un-contamination, un-contamination to moderate contamination, moderate contamination, moderate to heavy contamination, heavy contamination, heavy to extreme contamination, and extreme contamination are the contamination categories with  $I_{geo}$  values equal to or less than zero ( $I_{geo} \leq 0$ ), between  $0 < I_{geo} \leq 1$ , between  $1 < I_{geo} \leq 2$ , between  $2 < I_{geo} \leq 3$ , between  $3 < I_{geo} \leq 4$ , between  $4 < I_{geo} \leq 5$ , and more than five ( $I_{geo} > 5$ ), respectively (Kusin et al., 2018). A high anthropogenic influence is indicated by a positive  $I_{geo}$  value.

*Enrichment factor*

The *EF* index model in Eq. (4) was used to calculate the degree of HM contamination caused by human inputs in the area.

$$EF = \frac{(C_n/C_{ref})_{sample}}{(C_n/C_{ref})_{background}} \tag{4}$$

where  $C_n$  represents the concentration (mg/kg) of each studied HM in surface soil, and  $C_{ref}$  represents the concentration of reference metal (mg/kg). Among the HMs, scandium (Sc), Mn, titanium (Ti), Al, and Fe are commonly used as reference HMs in the earth’s crust (Jiang et al., 2017); however, in this study, the concentration of Fe was chosen as a reference metal for geochemical normalization because: (1) it founded mostly in combination with very fine surfaces of solids, (2) it has similar geochemistry to most of the earth HMs, and (3) it has a consistent trend of natural occurrence. The *EF* values less than ( $EF < 1$ ) represent no enrichment, the *EF* values between  $1 < EF < 3$  represent minor enrichment, the *EF* values between  $3 < EF < 5$  represent moderate enrichment, the *EF* values between  $5 < EF < 10$  represent moderately to severe enrichment, the *EF* values between  $10 < EF < 25$  represent severe

enrichment, the *EF* values between  $25 < EF < 50$  represent very severe enrichment, and the *EF* values more than fifty ( $EF > 50$ ) represent extremely severe enrichment, were adopted as the potential levels of soil enrichment in terms of HM pollution (ur Rehman et al., 2018).

Environmental hazard assessment

*Potential ecological hazard*

The potential ecological hazard index (*PEHI*) model (Eq. (5)), first developed by Hakanson (1980), was used as a technique in this study to encompass a diversity of research realms and assess ecological threats triggered by the concerned HMs (Chen et al., 2015; Wu et al., 2015).

$$PEHI = \sum_i^n E_r^i = \sum_i^n T_r^i \times \frac{C^i}{C_n^i} \tag{5}$$

where *PEHI* is a composite index, representing the possible ecological hazard of all the HMs examined in soil,  $E_r^i$  is the potential ecological hazard of *i*th HM,  $T_r^i$  is the toxic response factor value 2, 1, 5, 5, 5, 1, 30, 40, and 5 for Cr, Mn, Co, Ni, Cu, Zn, Cd, Hg, and Pb, respectively,  $C^i$  is the detected concentration and  $C_n^i$  is the threshold value of each HMs tested in soil (Hakanson, 1980; ur Rehman et al., 2018). The *PEHI* values  $< 95$ , between  $95 < PEHI < 190$ , between  $190 < PEHI < 380$ , and more  $> 380$ , respectively, represent low, moderate, considerable, high, and very high ecological hazard triggered by the concerned HMs, whereas the  $E_r^i$  values graded as less than 40 ( $E_r^i < 40$ ), between  $40 < E_r^i < 80$ , between  $80 < E_r^i < 160$ , between  $160 < E_r^i < 320$ , and more than 320 ( $E_r^i > 320$ ) represent a low, moderate, considerable, high, and very serious ecological hazard, respectively, in the study area (Hakanson, 1980).

*Human hazard index*

Population exposure to polluted HM soil by ingestion, inhalation, and skin contact may result in both non-cancer and cancer toxicity, depending on exposed metal concentration in surface soil (Huang et al., 2018). To estimate the potential hazard of HMs, the following models (Eqs. 6–13) developed by the USEPA (Agerncy, 2002; US Environmental Protection



Agency, 1999) were applied both to dependent adults and children populations (ur Rehman et al., 2018).

$$ADIng = C \times \frac{IngR \times EF \times ED}{BW \times AT} \times 10^{-6} \quad (6)$$

$$ADInh = C \times \frac{InhR \times EF \times ED}{PEF \times BW \times AT} \quad (7)$$

$$ADIderm = C \times \frac{SA \times AF \times ABS \times EF \times ED}{BW \times AT} \times 10^{-6} \quad (8)$$

where  $ADIng$ ,  $ADInh$ , and  $ADIderm$  reflect the ADIs of HMs (mg/kg/day) by soil ingestion, inhalation, and dermal contact, respectively,  $C$  represents the concentration of HM in soil,  $IngR$  (mg/day) and  $InhR$  ( $m^3$ /day) represent the surface soil ingestion and inhalation rates, respectively,  $EF$  represents the exposure frequency in per day/year,  $ED$  represents the exposure duration in per year,  $SA$  represents the exposed skin surface area in  $cm^2$ ,  $AF$  represents the skin adherence factor in  $kg/m^2$ /day,  $ABS$  represents the dermal absorption factor,  $PEF$  represents the particle emission factor in  $m^3/kg$ ,  $BW$  represents the body weight in kg, and  $AT$  stands for average time in per day (Table S2).

Further, to evaluate the non-carcinogenic hazard of Cr, Mn, Co, Ni, Cu, Zn, Cd, Hg, Pb, Fe, and Al for each receptor group, the hazard quotient ( $HQ$ ) and hazard index ( $HI$ ) models (Eqs. 9–12) were utilized for selected pathways separately (Jia et al., 2018).

$$HQing = \frac{ADIng}{RfD} \quad (9)$$

$$HQinh = \frac{ADInh}{RfD} \quad (10)$$

$$HQderm = \frac{ADIderm}{RfD} \quad (11)$$

$$HI = \sum HQ \quad (12)$$

where  $HQing$ ,  $HQinh$ , and  $HQderm$  represent the  $HQ$  of individual HMs via soil ingestion, inhalation, and skin contact, respectively, where  $RfD$  is the oral toxicity reference dose  $3.00E-03$ ,  $1.4E-01$ ,  $1.4E-03$ ,  $2.00E-02$ ,  $3.7E-02$ ,  $3.00E-01$ ,  $5.00E-04$ ,  $1.00E-03$ ,  $3.6E-03$ ,  $7.00E-01$ , and  $4.00E-04$  mg/kg/day of individual Cr,

Mn, Co, Ni, Cu, Zn, Cd, Hg, Pb, Fe, and Al, respectively (USEPA, 2005). The  $\sum HQ$  ( $HI$ ) evaluates the entire non-carcinogenic hazard posed by all the detected HMs, its value of more than one ( $HI > 1$ ) suggests potential non-carcinogenic impacts of HMs to exposed individual, while its value of less than one ( $HI < 1$ ) indicates the lowest toxicity of HMs having potential detrimental health effects on the dependent population (Kusin et al., 2018).

HMs like Cr, Cd, and Pb are carcinogenic, and their long-term exposure might result in an incremental lifetime cancer hazard ( $ILCH$ ). Its overall individual HM cancer hazard was calculated using Eq. (13) by multiplying individual HM lifetime average daily intake ( $LADI$ ) with their respective cancer slope factor ( $SF$ , mg/kg/day) (Kumar et al., 2013).

$$ILCH = LADI \times SF \quad (13)$$

Table S2 of the supplementary materials lists all of the exposure variables utilized in the aforementioned non-carcinogenic and carcinogenic hazard assessments.

## Statistics

In this study, the computer packages including Microsoft Excel (V16.0) and Statistical Package for Social Sciences (IBM-SPSS-23; Inc., Chicago, IL, USA) were used to statistically analyzed the instrumental data for arithmetic mean, minimum, maximum, range, standard deviation, and normal distribution test etc., where the manuscript interactive scientific graphing and data analysis were portrayed using Origin Pro V9.0 (Northampton, MA, USA). Besides, multivariate statistical analyses, e.g., principal component analysis (PCA) with Varimax Kaiser normalization techniques was employed to discern the possible sources of HM contaminations in surface soil, while the Arc-GIS (ArcGIS-10.5, ESRI Inc., USA) spatial interpolation techniques were used to spatially display the data distribution and draw the grid-based contouring maps.

## Results and discussion

### Concentration of heavy metals in surface soil

The detailed descriptive statistics of Cr, Mn, Co, Ni, Cu, Zn, Cd, Hg, Pb, Fe, and Al concentrations (mg/

kg) in surface soil along the basin of River Swat, Khyber Pakhtunkhwa, Pakistan, are summarized in Tables 1 and S2. There was significant variation ( $p < 0.05$ ) in the concentrations of individual HMs along with the sampling sites. The overall mean HM concentrations were the most abundant for Al (24,730.19 mg/kg), followed by Fe (22,419.41 mg/kg) > Mn (386.78 mg/kg) > Zn (57.75 mg/kg) > Cr (38.07 mg/kg) > Ni (32.46 mg/kg) > Cu (23.43 mg/kg) > Pb (19.59 mg/kg) > Co (10.77 mg/kg) > Cd (3.18 mg/kg) > Hg (0.12 mg/kg), which corresponded to their abundance in the earth crust. In comparison to the rest of the HMs, the concentrations of Cd, Hg, Fe, and Al in the collected soil samples were substantially higher than their respective background values (Jia et al., 2018). However, the concentrations of Cr and Mn in 5.45% each, Co in 10.90%, Zn in 27.27%, Cu in 36.36%, Ni in 41.81%, and Hg in 92.72% of the total soil samples exceeded their respective background values (Han et al., 2018; Meng et al., 2016), whereas the concentration Pb was noticed within their background value. These high loadings of HM in comparison to its respective background values might be the result of human activity in the region.

Furthermore, the overall quantity of each examined metal in surface soil was within its maximum permissible

limit (MPL), except for Ni and Cd, which might be harmful to dependent human health, as per SEPA (2005) and EU (2006) guidelines (Guan et al., 2018; Liang et al., 2017) (Tables 1 and S3). The overall concentrations of targeted HM pollution in soil varied greatly based on the standard deviation (SD) and coefficient of variance (CV). A CV value of less than 20% suggests minimal Al and Fe fluctuation; a value between 21% < CV ≤ 50% designates moderate variability of Cr, Co, Pb, Ni, Cu, and Mn; and a value between 51% < CV ≤ 100% indicates high variability of Zn, Hg, and Cd, which may be due to human (agronomic practices) effect in the region; however, no metal was detected in very high variability (CV > 100%) (Table 1). HM pollution with a low CV value revealed potential natural pollution resources in the vicinity, whereas high CV value pollution is mostly generated by nearby anthropogenic activities (Baltas et al., 2020; Mamut et al., 2017). The kurtosis and skewness statistical indices used to determine the normality or abnormality of contaminated HM distribution revealed that Cu, Ni, Mn, Cd, Fe, Zn, and Pb contaminations in the area surface soil were normally distributed with skew values ranging from 1 to -1 (Table 1), whereas the supply of Al, Co, and Cr into surrounding soil indicates abnormality with slightly positive skewness values (Baltas et al., 2020; Chandrasekaran et al., 2015; Pan et al., 2017).

**Table 1** Descriptive statistics of heavy metal concentrations (mg/kg) in surface soil samples (n=55) collected along the basin of River Swat, Khyber Pakhtunkhwa, Pakistan

Statistics	Cr	Mn	Co	Ni	Cu	Zn	Cd	Hg	Pb	Fe	Al
Min	14.42	170.40	3.79	14.15	9.41	14.13	0.07	0.05	5.48	17,341.11	18,022.08
Max	90.16	754.38	30.80	60.40	51.26	129.18	9.11	0.39	31.88	29,845.31	39,996.71
Mean	38.07	386.78	10.75	32.46	23.43	57.75	3.18	0.12	19.59	22,419.41	24,730.19
Median	32.98	396.87	10.07	29.95	22.85	52.39	3.11	0.09	20.60	21,981.11	23,755.02
SD	17.59	114.26	4.75	11.44	8.55	30.67	1.98	0.07	7.41	2798.81	4549.52
Range	75.74	583.98	27.01	46.25	41.85	115.05	9.04	0.34	26.40	12,504.20	21,974.63
CV %	46.20	29.54	44.18	37.24	36.49	53.10	62.26	58.33	37.82	12.48	18.39
*MPL	100.00	2000.00	50.00	50.00	100.00	300.00	3.00	1.00	100.00	50,000.00	-
Skewness	1.35	0.91	1.86	0.93	0.97	0.42	0.78	2.09	-0.12	0.45	1.68
Kurtosis	1.43	1.49	5.55	0.26	2.19	-0.90	0.81	5.27	-1.33	-0.14	3.25
**Background	80.00	615.00	15.00	32.00	26.00	80.00	0.11	0.06	32.00	38.90	78.10

Min minimum, Max maximum, Mean arithmetic mean, SD standard deviation, CV (%) coefficient of variance, MPL maximum permissible limit

\*SEPA (2005), FAO/WHO (2011), and EU (2006)

\*\*Jia et al. (2018)

Heavy metal spatial distribution patterns and their probable source apportionment along the River Swat basin

The spatial distribution of HM contaminations in surface soil of the study area was mapped with Arc-GIS using the conventional kriging interpolation method (Fig. 2a). Multiple anthropogenic and natural factors were examined throughout the geostatistical procedures

to determine the distribution patterns of the studied HM contaminations along with the sample locations. The results of multivariate PCA exposed variability of HM contaminations with eigenvalues greater than 1 along the basin in three components with a total variance of 71.316% and relative contributions of rotational principal component-1 (PC-1)—28.67%, PC-2—26.98%, and PC-3—15.67% (Fig. 2b and Table S4). The PC-1's substantial (>0.7) positive loading for Al, Fe, and Mn, as

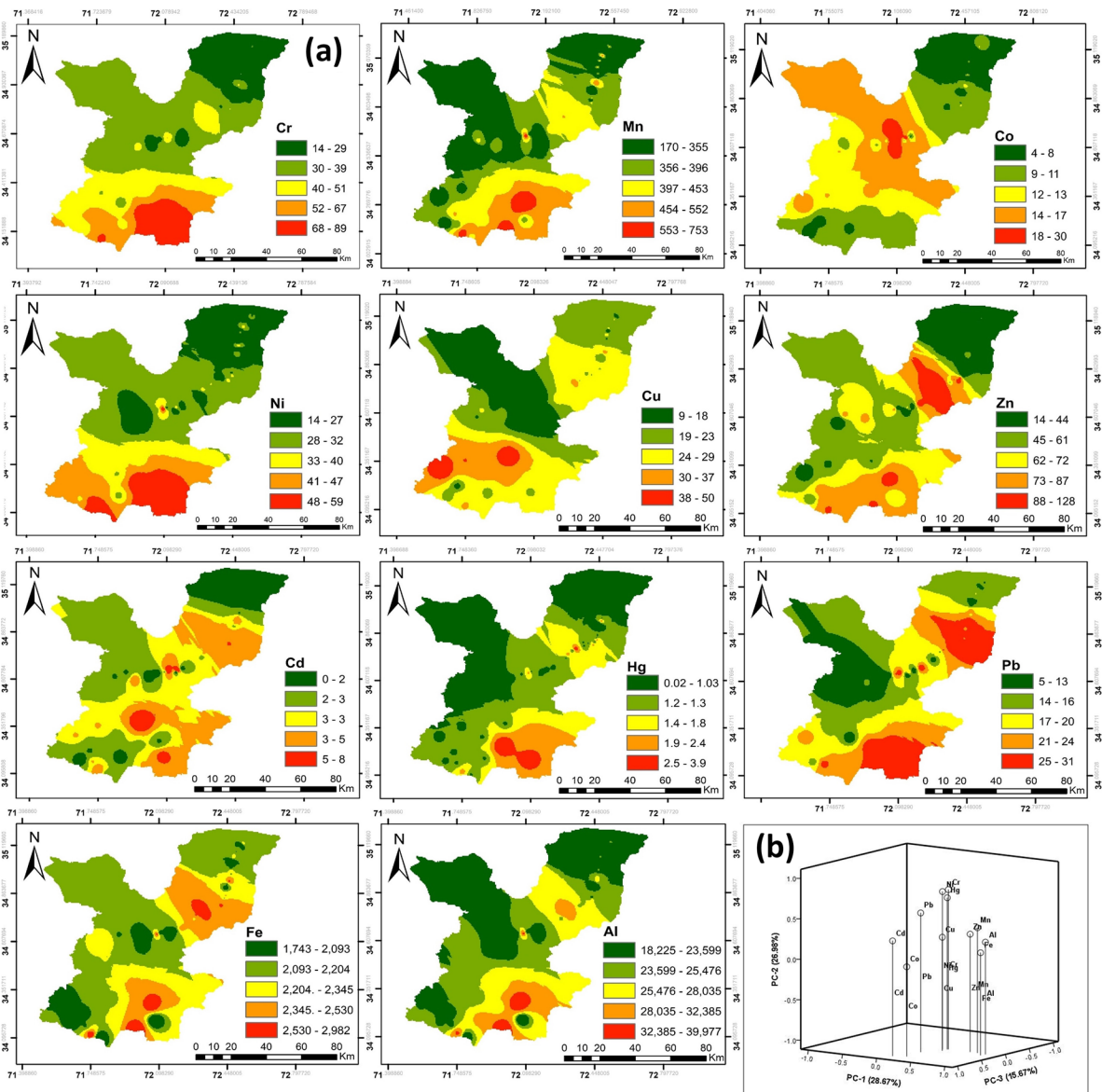


**Fig. 2** a Geographical distribution of heavy metal (HM) concentrations (mg/kg) and b total variance and rotated component matrix of individual HMs in surface soil of the River Swat basin



well as moderate (0.5–0.7) loading for Zn, may be better explained by natural lithogenic processes, suggesting that Al, Fe, and Mn are the product of geochemical weathering of source rock material (Baltas et al., 2020; Chandrasekaran et al., 2015), whereas the Zn loading was recommended to be a mixed source of lithogenic and anthropogenic input, occurring predominantly in animal dung and phosphate fertilizers used in agricultural operations (Marrugo-Negrete et al., 2017). Similarly, in the PC-2 a substantial (>0.7) positive loading for Cr, Ni, and Hg was also seen (Fig. 2b and Table S4). The high loading of Cr and Ni most likely resulted from the parent minerals during soil history, whereas the Hg contamination may have both natural and human causes. Likewise, the PC-3 had a strong (>0.7) factor loading on Cd and Co only (Fig. 2b and Table S4), despite its relative abundance of 15.67%, indicating that this contamination in the riverine basin might be owing to both human and geogenic origins (Barceloux & Barceloux, 1999; Khan et al., 2013a). This overall HM contamination along the studied basin was influenced not only by local geology but also by anthropogenic inputs such as industrial discharge, agrofertilizers, and commercial and home sewages, all of which released harmful chemicals into the environment. The usage of such wastewater in agriculture irrigation is a popular and common practice since it provides nutritious components while reducing fertilizer cost. However, long-term irrigation with municipal/industrial wastewater, on the other hand, not only degrades soil quality but also causes phytotoxicity, human health, and environmental issues in the region.

### Heavy metal pollution evaluation

Among the overall HMs, the *CF* of Fe, Al, and Cd were significantly high followed by Hg>Ni>Cu>Co>Zn>Mn>Pb>Cr (Table S5). The mean *CF* values for Fe and Al indicated a very high degree of pollution in the area, whereas for Cd its value suggested a considerable contamination level, and for the rest of HMs its values stayed in the range of very low pollution level (Fig. 3a). Out of 55 samples, 92% of the total samples reflected substantial (*CF*>6) pollution, 6% considerable (3<*CF*<6) pollution, and 2% reflected very low contamination (*CF*<1) around the basin (Table S5). The high Fe and Al pollution in the area might be due to the natural availability of Fe-Al ore deposits, which make them more mobile than other HMs and allow them to quickly leach out of surrounding source materials (Rose et al., 1979).

Further, to simplify the overall pollution control, the *CF* values of the studied HMs were summed to calculate the *CD* of HMs along with the basin (Table S5). The collective *CD* of Fe and Al along the sampling sites were recorded comparatively very high (676.56–1279.35), whereas the *CD* of Cr, Mn, Co, Ni, Cu, Zn, As, Cd, Hg, and Pb ranged between 3.27 and 90.61 (Table S5). Along with the sampling sites, 18% of the total upstream sample sites showed low to a considerable degree of contamination (6<*CD*<24), whereas the remaining 82% of the total downstream sites showed a high degree of contamination (*CD*>24), suggesting alarming anthropogenic pollution inputs along the River Swat basin (Table S5).

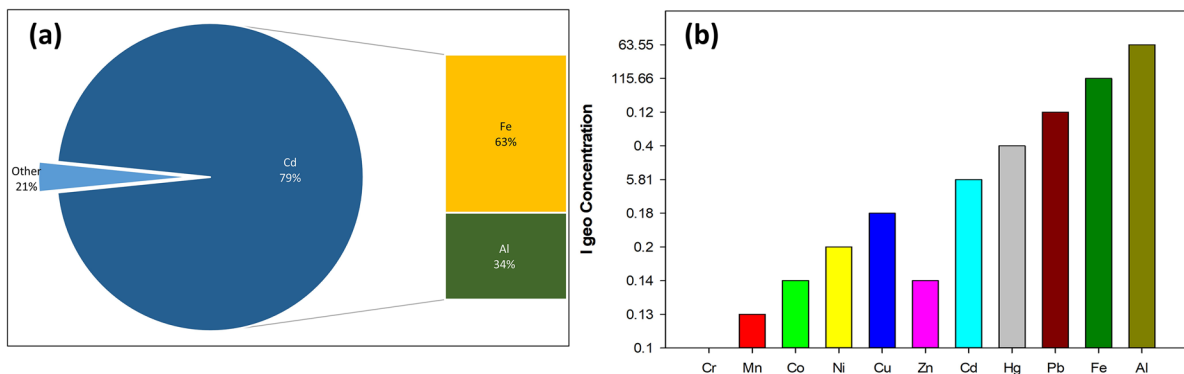


**Fig. 3** a Average individual heavy metal (HM) contamination factor (*CF*) and their collective contamination degree. b Average geo-accumulation indices ( $I_{geo}$ ) of individual HMs in the study area

The average  $I_{geo}$  values of this study revealed that HMs were un-contaminated to extremely contaminated in order of  $Fe > Al > Cd > Hg > Ni > Cu > Zn > Co > Mn > Pb > Cr$  (Fig. 3b). Along with the sample locations, the mean  $I_{geo}$  values of Cr, Mn, Co, Ni, Cu, Zn, Hg, and Pb were found to be less than one, while those of Cd, Fe, and Al were found to be comparatively very high ( $I_{geo} > 5$ ). However, the overall values of geo-accumulation on the Müller scale indicate that the soil in this basin are uncontaminated to moderately polluted ( $0 < I_{geo} \leq 1$ ) with Cr, Mn, Co, Ni, Cu, Zn, Hg, and Pb, and moderately to extremely polluted ( $1 < I_{geo} > 5$ ) with Cd, Fe, and Al (Table S6). The values of  $EF$  varying from 0.5 to 1.5 indicate that the pollution generated by the corresponding metal is the result of probable geogenic activities, while  $EF$  values greater than 1.5 ( $EF > 1.5$ ) indicate that HMs under consideration are of human origin (ur Rehman et al., 2018). In this study, the average  $EF$  values (Table S7) for individual Cr, Mn, Co, Zn, and Pb were less than 1.5 ( $EF < 1.5$ ), indicating that these HMs came from surrounding natural sources in the area and belonged to the parent materials, whereas for Ni, Cu, Cd, Hg, Fe, and Al, the values of  $EF$  were greater than 1.5, indicating nearby anthropogenic impacts. As per the scale, the overall mean  $EF$  values of Cr were less than 1 ( $EF < 1$ ) signifying no enrichment of Cr in the area; the  $EF$  values for Mn, Co, Ni, Cu, Zn, and Pb were between  $1 < EF < 3$  indicating minor enrichment

of Mn, Co, Ni, Cu, Zn, and Pb; the  $EF$  values for Hg were between  $3 < EF < 5$ , suggesting a moderate enrichment of Hg; the  $EF$  values for Cd were between  $25 < EF < 50$  indicating a very severe enrichment of Cd; and the  $EF$  values for Fe and Al were more than 50 ( $EF > 50$ ) indicating extremely severe enrichment Fe and Al along with the monitoring sites of River Swat basin (Table S7).

#### Potential ecological hazard

Table S8 and Fig. 4 summarize the overall PEHIs of HMs in surface soil, evaluated in terms of  $E_r^i$  of individual HM. The spatial distribution of PEHIs along the sample locations varied from low to considerable hazard ( $< 95 < PEHI < 190$ ) (Fig. 4a), with Cd having the highest average  $E_r^i$  (51%), followed by Hg > Ni > Co > Pb > Cu > Cr > Zn > Mn (Fig. 4b). Along with the basin soil, the PEHIs of the sampling site ranged between 10.87 and 299.66 with a mean value of 121.40 and a total sum of 6329.60 (Table S8). The overall trend of ecological hazard showed potential ups and downs along with the sites from low to considerable hazard. At sites S1–S11 and S13, the calculated PEHIs were estimated to be at low ecological hazard ( $PEHI < 95$ ), whereas at sites S22, S26, S32, S34, S45, and S47 the hazard was considerable ( $190 < PEHI < 380$ ), and at the rest of the sampling locations the potential ecological hazard was

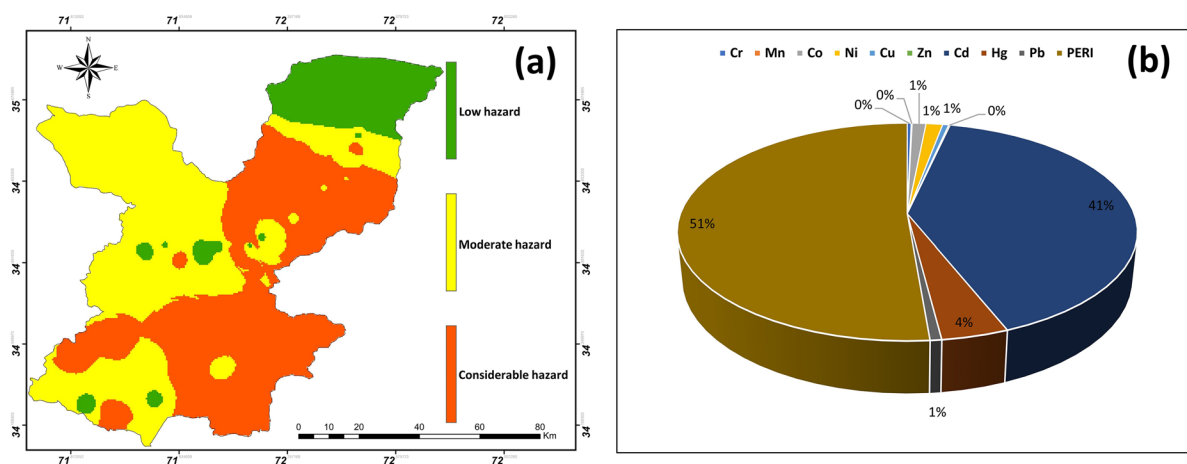


**Fig. 4** **a** Spatial distribution of potential ecological hazard index ( $PEHI$ ) values of combined heavy metal contaminations. **b** Single metal ecological hazard ( $E_r^i$ ) values and its percentage (%) contributions to combined metal PEHIs

moderate ( $95 < PEHI < 190$ ) (Table S8 and Fig. S1). Besides, the individual  $E_r^i$  values for Cr, Mn, Co, Ni, Cu, Zn, Hg, and Pb in the soil of the study area were within the normal range ( $E_r^i < 40$ ), suggesting low ecological hazard along with the sampling sites,

except for Cd whose  $E_r^i$  values significantly fluctuated between 2.10 and 273.31 with a mean value of 95.53 and a total sum of 5254.05, suggesting considerable ecological hazard factor in the area ( $80 < E_r^i < 160$ ) (Table S8).

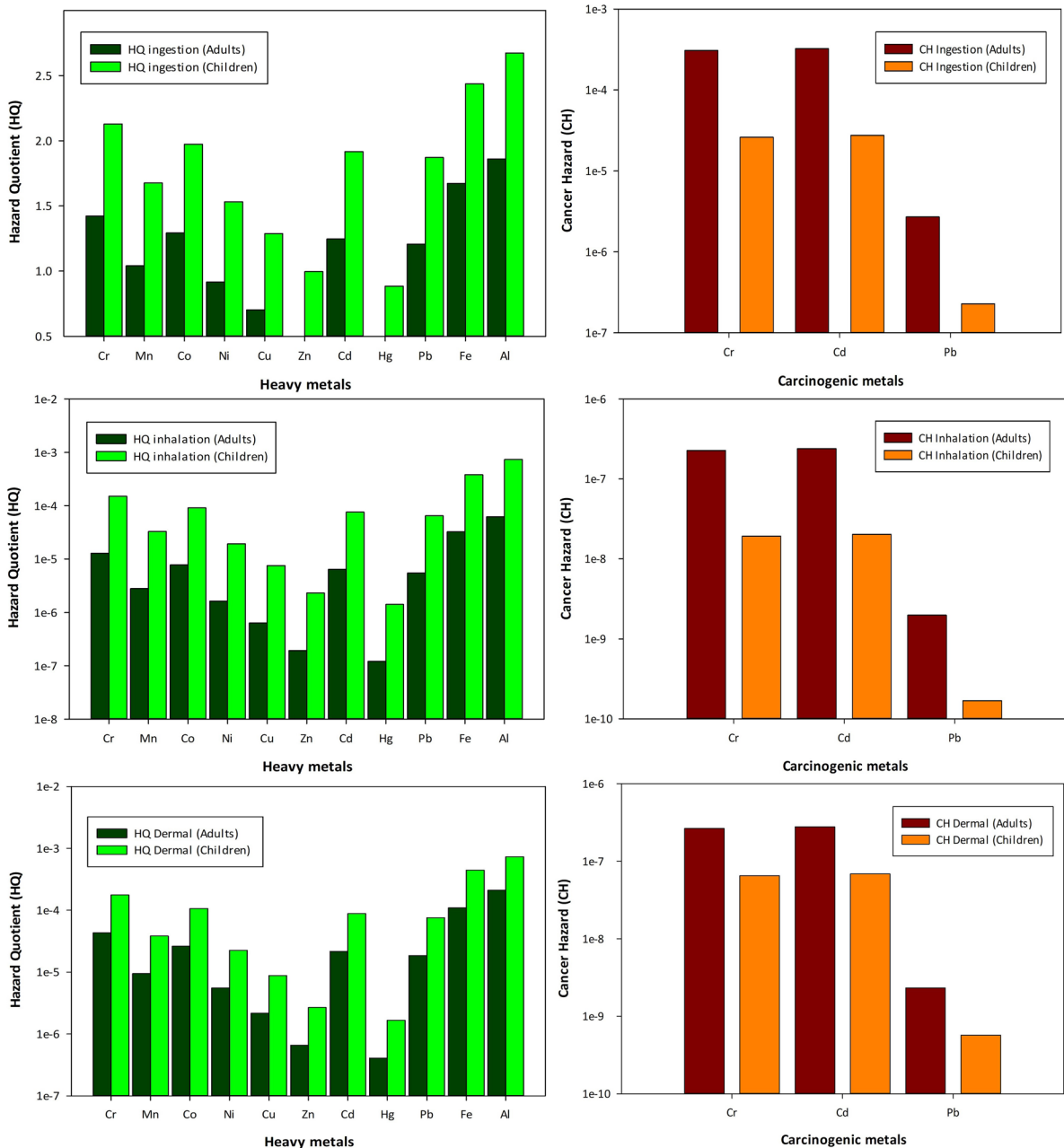


**Fig. 5** Heavy metals’ non-carcinogenic and carcinogenic hazards posed by the area’s human adults and children population via soil ingestion, inhalation, and skin contact

## Potential human health hazard

The statistics of non-carcinogenic and carcinogenic hazards of HM exposure in surface soil via non-dietary intake and inhalation, as well as skin contact, in adults and children's demographic groups were illustrated in Fig. 5 and Tables S9-S11. The overall distributions of  $\sum$ ADI of HMs along the monitoring sites through all exposer routes were ranked in order of  $Al > Fe > Mn > Zn > Cr > Ni > Cu > Pb > Co > Cd > Hg$  (Table S9). The total non-carcinogenic ADIs of the tested HMs were found to be higher in children than adult population. Furthermore, the route of oral ingestion was identified as a potentially significant way for soil HM absorption into the human body, followed by dermal interaction and inhalation. The resulted HQs of HMs were peaked for Al followed by  $Fe > Cr > Co > Cd > Pb > Mn > Ni > Cu > Zn > Hg$  irrespective of adults and children via all exposure pathways (Fig. 5 and Table S10). Among the exposure routes, oral intake for both adults and children has been identified as the most common pathway for HMs to harm human health. Besides, the adult's and children's non-carcinogenic HIs of HMs in the study area were ranged from  $6.23E-05$  to  $4.24E-01$  and  $7.35E-04$  to  $1.62E+00$ , respectively (Table S10). The overall non-carcinogenic hazards of HMs in the study area for adults were not significant ( $HI < 1$ ), but their values for children exceed the safe limit ( $HI > 1$ ), indicating that the tested HMs may have non-carcinogenic effects in children exposed more than adults based on multiple factors (EPA, 2012). However, the total HIs of each HM's toxicity was calculated to be higher for children than adults in the declining order of  $Hg < Zn < Cu < Ni < Mn < Pb < Cd < Co < Cr < Fe < Al$  (Fig. S2). Furthermore, the ILCHs of Cr, Cd, and Pb in long-term exposed individuals were estimated to assess the total carcinogenic hazard from surface soil ingestion, inhalation, and dermal contact (Fig. 5 and Table S11). The  $\sum$ ILCHs of Cr, Cd, and Pb for dependent adults and children varied significantly from  $7.75E-09$  to  $1.41E-04$  and  $9.17E-08$  to  $1.66E-03$ , respectively. The Cd intake by all exposed routes contributes much more to the  $\sum$ ILCH in children than in adults, followed by Cr and Pb. Further, the range of overall carcinogenic hazard of HMs in the area was within the USEPA acceptable range ( $1 \times 10^{-7}$ – $1 \times 10^{-4}$ ), indicating no major long-term health impacts. However, in terms of both projected carcinogenic and non-carcinogenic hazard, children were more vulnerable than the area's reliant adult population.

## Conclusions

This study investigated the ecological and human health concerns induced by HM-contaminated soil using various UpToDate indices based on high-spatial-resolution sampling. The overall contaminations of Cr, Mn, Co, Zn, Cu, Ni, Hg, Fe, and Al in the riverine basin soil of River Swat, Pakistan, varied significantly between sampling sites and exceeded their respective background values set by SEPA (2005), FAO/WHO (2011), and EU (2006). As per HM pollution evaluation indices, the overall CF of Fe, Al, and Cd was substantially high, followed by  $Hg > Ni > Cu > Co > Zn > Mn > Pb > Cr$ , with 92% substantial ( $CF > 6$ ), 6% considerable ( $3 < CF < 6$ ), and 2% very low contamination ( $CF < 1$ ) of the total soil samples. Along with the basin, 18% of the total sampling sites had a low to a considerable degree of HM contamination ( $6 < CD < 24$ ), while the remaining 82% had a high degree of contamination ( $CD > 24$ ), suggesting likely anthropogenic sources of HM contamination in the area. As per potential toxicity concerns, the trend of ecological hazard showed potential ups and downs from low to considerable hazard ( $< 95 < PEHI < 190$ ), whereas for human health the potential carcinogenic hazard from HMs was within the USEPA acceptable range ( $1 \times 10^{-7}$ – $1 \times 10^{-4}$ ), but the non-carcinogenic hazard for children was substantial ( $HI > 1$ ), because they are more exposed than adults. Therefore, to properly track and reduce the HM contaminations caused by anthropogenic activities, as well as to mitigate their potential toxicity, this study suggests appropriate monitoring and environmental protection measures/strategies for global environmental protection agencies to control HM pollution in the environment and to protect the food chain from HM contamination.

**Acknowledgements** This study was supported by the Researchers Supporting Project number [RSP-2021/100], King Saud University, Riyadh, Saudi Arabia, and the Chinese Academy of Sciences (CAS)—President's International Fellowship Initiative (PIFI) post-doctoral fellowship. The authors appreciate the help with the Arc-GIS application from Mr. Muhammad Sohail, Department of Geography and Geomatics, University of Peshawar, and the clarity and writing style suggestions from Mr. Rafiullah, Department of English and Foreign Languages, University of Swat, Pakistan.

**Author contribution** All authors contributed to the study conception and design, material preparation, data collection, and analysis. The first draft of the manuscript was written by Kifayatullah Khan and Abdul Mohsin and all authors

commented on previous versions of the manuscript. All authors read and approved the final manuscript.

**Availability of data and materials** Possible resultant data supporting the findings of this study are accessible in the Supplemental Information, where the additional data that support the findings of this study will be made available upon request from the corresponding author.

**Declarations**

**Ethics approval and consent to participate** This is an observational study and does not involve any human subjects. The concerned University of Swat Research Ethics Committee has confirmed that no ethical approval is required.

**Consent for publication** Not applicable.

**Competing interests** The authors declare no competing interests.

**References**

Agerncy, U. E. P. (2002). *Supplemental guidance for developing soil screening levels far superfund sites*. Office of Solid Waste and Emergency Response.

Agomuo, E. N., & Amadi, P. U. (2017). Accumulation and toxicological risk assessments of heavy metals of top soils from markets in Owerri, Imo state, Nigeria. *Environmental Nanotechnology, Monitoring & Management*, *8*, 121–126.

Baltas, H., Sirin, M., Gökbayrak, E., & Ozcelik, A. E. (2020). A case study on pollution and a human health risk assessment of heavy metals in agricultural soils around Sinop province, Turkey. *Chemosphere*, *241*, 125015.

Barceloux, D. G., & Barceloux, D. (1999). Cobalt. *Journal of Toxicology: Clinical Toxicology*, *37*, 201–216.

Bing, H., Zhou, J., Wu, Y., Wang, X., Sun, H., & Li, R. (2016). Current state, sources, and potential risk of heavy metals in sediments of Three Gorges Reservoir, China. *Environmental Pollution*, *214*, 485–496.

Cai, L.-M., Xu, Z.-C., Qi, J.-Y., Feng, Z.-Z., & Xiang, T.-S. (2015). Assessment of exposure to heavy metals and health risks among residents near Tonglushan mine in Hubei, China. *Chemosphere*, *127*, 127–135.

Chandrasekaran, A., Ravisankar, R., Harikrishnan, N., Satapathy, K., Prasad, M., & Kanagasabapathy, K. (2015). Multivariate statistical analysis of heavy metal concentration in soils of Yelagiri Hills, Tamilnadu, India-Spectroscopical approach. *Spectrochimica Acta Part A: Molecular and Biomolecular Spectroscopy*, *137*, 589–600.

Chen, H., Teng, Y., Lu, S., Wang, Y., & Wang, J. (2015). Contamination features and health risk of soil heavy metals in China. *Science of the Total Environment*, *512*, 143–153.

Chen, L., Zhou, S., Shi, Y., Wang, C., Li, B., Li, Y., & Wu, S. (2018). Heavy metals in food crops, soil, and water in

the Lihe River Watershed of the Taihu Region and their potential health risks when ingested. *Science of the Total Environment*, *615*, 141–149.

Chen, Y., Li, T.-Q., Han, X., Ding, Z.-L., Yang, X.-E., & Jin, Y.-F. (2012). Cadmium accumulation in different pakchoi cultivars and screening for pollution-safe cultivars. *Journal of Zhejiang University Science B*, *13*, 494–502.

EPA, U. (2012). 2012 edition of the drinking water standards and health advisories. EPA 822-S-12-001.

European Union (EU). (2006). Commission Regulation (EC) No. 1881/2006 setting maximum levels for certain contaminants in foodstuffs. *Official Journal of European Union*, *364*, 5–24.

Facchinelli, A., Sacchi, E., & Mallen, L. (2001). Multivariate statistical and GIS-based approach to identify heavy metal sources in soils. *Environmental Pollution*, *114*, 313–324.

FAO/WHO. (2011). Joint Food and Agriculture Organization of the World Health Organization (FAO/WHO) Food Standards Programme Codex Committee on Contaminants in Foods. Fifth Session CF/5 INF/1, 21–25 March 2011. The Hague, The Netherlands.

Gu, Y. G., Li, Q. S., Fang, J. H., He, B. Y., Fu, H. B., & Tong, Z. J. (2014). Identification of heavy metal sources in the reclaimed farmland soils of the Pearl River estuary in China using a multivariate geostatistical approach. *Ecotoxicology and Environmental Safety*, *105*, 7–12.

Guan, Q., Wang, F., Xu, C., Pan, N., Lin, J., Zhao, R., Yang, Y., & Luo, H. (2018). Source apportionment of heavy metals in agricultural soil based on PMF: A case study in Hexi Corridor, northwest China. *Chemosphere*, *193*, 189–197.

Hakanson, L. (1980). An ecological risk index for aquatic pollution control. A Sedimentological Approach. *Water Research*, *14*, 975–1001.

Han, W., Gao, G., Geng, J., Li, Y., & Wang, Y. (2018). Ecological and health risks assessment and spatial distribution of residual heavy metals in the soil of an e-waste circular economy park in Tianjin, China. *Chemosphere*, *197*, 325–335.

Hu, Y., & Cheng, H. (2013). Application of stochastic models in identification and apportionment of heavy metal pollution sources in the surface soils of a large-scale region. *Environmental Science & Technology*, *47*, 3752–3760.

Huang, Y., Chen, Q., Deng, M., Japenga, J., Li, T., Yang, X., & He, Z. (2018). Heavy metal pollution and health risk assessment of agricultural soils in a typical peri-urban area in southeast China. *Journal of Environmental Management*, *207*, 159–168.

Iqbal, J., Saleem, M., & Shah, M. H. (2016). Spatial distribution, environmental assessment and source identification of metals content in surface sediments of freshwater reservoir, Pakistan. *Chemie Der Erde-Geochemistry*, *76*, 171–177.

Islam, M. S., Ahmed, M. K., Raknuzzaman, M., Habibullah-Al-Mamun, M., & Islam, M. K. (2015). Heavy metal pollution in surface water and sediment: A preliminary assessment of an urban river in a developing country. *Ecological Indicators*, *48*, 282–291.

Jia, Z., Li, S., & Wang, L. (2018). Assessment of soil heavy metals for eco-environment and human health in a rapidly urbanization area of the upper Yangtze Basin. *Scientific Reports*, *8*, 3256.



- Jiang, Y., Chao, S., Liu, J., Yang, Y., Chen, Y., Zhang, A., & Cao, H. (2017). Source apportionment and health risk assessment of heavy metals in soil for a township in Jiangsu Province, China. *Chemosphere*, *168*, 1658–1668.
- Kabata-Pendias, A. (2000). *Trace elements in soils and plants*. CRC Press.
- Kang, X., Song, J., Yuan, H., Duan, L., Li, X., Li, N., Liang, X., & Qu, B. (2017). Speciation of heavy metals in different grain sizes of Jiaozhou Bay sediments: Bioavailability, ecological risk assessment and source analysis on a centennial timescale. *Ecotoxicology and Environmental Safety*, *143*, 296–306.
- Khan, K., Khan, H., Lu, Y., Ihsanullah, I., Nawab, J., Khan, S., Shah, N. S., Shamshad, I., & Maryam, A. (2014). Evaluation of toxicological risk of foodstuffs contaminated with heavy metals in Swat, Pakistan. *Ecotoxicology and Environmental Safety*, *108*, 224–232.
- Khan, K., Lu, Y., Khan, H., Ishtiaq, M., Khan, S., Waqas, M., Wei, L., & Wang, T. (2013a). Heavy metals in agricultural soils and crops and their health risks in Swat District, northern Pakistan. *Food and Chemical Toxicology*, *58*, 449–458.
- Khan, K., Lu, Y., Khan, H., Zakir, S., Khan, S., Khan, A. A., Wei, L., & Wang, T. (2013b). Health risks associated with heavy metals in the drinking water of Swat, northern Pakistan. *Journal of Environmental Sciences*, *25*, 2003–2013.
- Khan, K., Younas, M., Sharif, H. M. A., Wang, C., Yaseen, M., Cao, X., Zhou, Y., Ibrahim, S. M., Yvette, B., & Lu, Y. (2022). Heavy metals contamination, potential pathways and risks along the Indus Drainage System of Pakistan. *Science of the Total Environment*, *809*, 151994.
- Khan, S., Rehman, S., Khan, A. Z., Khan, M. A., & Shah, M. T. (2010). Soil and vegetables enrichment with heavy metals from geological sources in Gilgit, northern Pakistan. *Ecotoxicology and Environmental Safety*, *73*, 1820–1827.
- Kumar, B., Verma, V. K., Kumar, S., & Sharma, C. S. (2013). Probabilistic health risk assessment of polycyclic aromatic hydrocarbons and polychlorinated biphenyls in urban soils from a tropical city of India. *Journal of Environmental Science and Health, Part A*, *48*, 1253–1263.
- Kusin, F. M., Azani, N. N. M., Hasan, S. N. M. S., & Sulong, N. A. (2018). Distribution of heavy metals and metalloid in surface sediments of heavily-mined area for bauxite ore in Pengerang, Malaysia and associated risk assessment. *CATENA*, *165*, 454–464.
- Li, Z., Ma, Z., van der Kuijp, T. J., Yuan, Z., & Huang, L. (2014). A review of soil heavy metal pollution from mines in China: Pollution and health risk assessment. *Science of the Total Environment*, *468*, 843–853.
- Liang, J., Feng, C., Zeng, G., Gao, X., Zhong, M., Li, X., Li, X., He, X., & Fang, Y. (2017). Spatial distribution and source identification of heavy metals in surface soils in a typical coal mine city, Lianyuan, China. *Environmental Pollution*, *225*, 681–690.
- Liu, J., Cao, L., & Dou, S. (2017). Bioaccumulation of heavy metals and health risk assessment in three benthic bivalves along the coast of Laizhou Bay, China. *Marine Pollution Bulletin*, *117*, 98–110.
- Mamut, A., Eziz, M., Mohammad, A., & Anayit, M. (2017). The spatial distribution, contamination, and ecological risk assessment of heavy metals of farmland soils in Karashahar-Baghrash oasis, northwest China. *Human and Ecological Risk Assessment: An International Journal*, *23*, 1300–1314.
- Marrugo-Negrete, J., Pinedo-Hernández, J., & Díez, S. (2017). Assessment of heavy metal pollution, spatial distribution and origin in agricultural soils along the Sinú River Basin, Colombia. *Environmental Research*, *154*, 380–388.
- Meng, W., Wang, Z., Hu, B., Wang, Z., Li, H., & Goodman, R. C. (2016). Heavy metals in soil and plants after long-term sewage irrigation at Tianjin China: A case study assessment. *Agricultural Water Management*, *171*, 153–161.
- Muhammad, S., Shah, M. T., & Khan, S. (2011). Heavy metal concentrations in soil and wild plants growing around Pb–Zn sulfide terrain in the Kohistan region, northern Pakistan. *Microchemical Journal*, *99*, 67–75.
- Muller, G. (1979). Heavy-metals in sediment of the Rhine—Changes since 1971. *Umschau in Wissenschaft Und Technik*, *79*, 778–783.
- Nawab, J., Khan, S., Shah, M. T., Khan, K., Huang, Q., & Ali, R. (2015). Quantification of heavy metals in mining affected soil and their bioaccumulation in native plant species. *International Journal of Phytoremediation*, *17*, 801–813.
- Pan, H., Lu, X., & Lei, K. (2017). A comprehensive analysis of heavy metals in urban road dust of Xi'an, China: Contamination, source apportionment and spatial distribution. *Science of the Total Environment*, *609*, 1361–1369.
- Qitong, X., & Mingkui, Z. (2017). Source identification and exchangeability of heavy metals accumulated in vegetable soils in the coastal plain of eastern Zhejiang province, China. *Ecotoxicology and Environmental Safety*, *142*, 410–416.
- Raychaudhuri, S. S., Pramanick, P., Talukder, P., & Basak, A. (2021). Polyamines, metallothioneins, and phytochelatins—Natural defense of plants to mitigate heavy metals. *Studies in Natural Products Chemistry*, *69*, 227–261.
- Rodrigues, S., Cruz, N., Coelho, C., Henriques, B., Carvalho, L., Duarte, A., Pereira, E., & Römken, P. F. (2013). Risk assessment for Cd, Cu, Pb and Zn in urban soils: Chemical availability as the central concept. *Environmental Pollution*, *183*, 234–242.
- Rose, A. W., Hawkes, H. E., Webb, J. S. (1979). *Geochemistry in mineral exploration*. Academic press London.
- Sani, H. A., Ahmad, M. B., Hussein, M. Z., Ibrahim, N. A., Musa, A., & Saleh, T. A. (2017). Nanocomposite of ZnO with montmorillonite for removal of lead and copper ions from aqueous solutions. *Process Safety and Environmental Protection*, *109*, 97–105.
- SEPA. (2005). The limits of pollutants in food. State Environmental Protection Administration, China (SEPA), GB 2762-2005.
- Shahid, M., Dumat, C., Khalid, S., Schreck, E., Xiong, T., & Niazi, N. K. (2017). Foliar heavy metal uptake, toxicity and detoxification in plants: A comparison of foliar and root metal uptake. *Journal of Hazardous Materials*, *325*, 36–58.
- Singh, U. K., & Kumar, B. (2017). Pathways of heavy metals contamination and associated human health risk in Ajay River basin, India. *Chemosphere*, *174*, 183–199.
- Stafilov, T., Šajn, R., Boev, B., Cvetković, J., Mukaetov, D., Andreevski, M., & Lepitkova, S. (2010). Distribution of

- some elements in surface soil over the Kavadarci region, Republic of Macedonia. *Environmental Earth Sciences*, *61*, 1515–1530.
- Sun, Y., Zhou, Q., Xie, X., & Liu, R. (2010). Spatial, sources and risk assessment of heavy metal contamination of urban soils in typical regions of Shenyang, China. *Journal of Hazardous Materials*, *174*, 455–462.
- Sungur, A., & Özcan, H. (2015). Chemometric and geochemical study of the heavy metal accumulation in the soils of a salt marsh area (Kavak Delta, NW Turkey). *Journal of Soils and Sediments*, *15*, 323–331.
- Tian, K., Hu, W., Xing, Z., Huang, B., Jia, M., & Wan, M. (2016). Determination and evaluation of heavy metals in soils under two different greenhouse vegetable production systems in eastern China. *Chemosphere*, *165*, 555–563.
- ur Rehman, I., Ishaq, M., Ali, L., Khan, S., Ahmad, I., Din, I.U., Ullah, H., (2018). Enrichment, spatial distribution of potential ecological and human health risk assessment via toxic metals in soil and surface water ingestion in the vicinity of Sewakht mines, district Chitral, Northern Pakistan. *Ecotoxicology and Environmental Safety*, *154*, 127–136.
- US Environmental Protection Agency. (1999). Cancer risk coefficients for environmental exposure to radionuclides. Office of Radiation and Indoor Air Federal Guidance Report No. 13 EPA-402-R.
- USEPA, M. (2005). Guidelines for carcinogen risk assessment. *Risk Assessment Forum US Environmental Protection Agency, Washington, DC EPA/630/P-03 F*.
- Wu, J., Lu, J., Li, L., Min, X., & Luo, Y. (2018). Pollution, ecological-health risks, and sources of heavy metals in soil of the northeastern Qinghai-Tibet Plateau. *Chemosphere*, *201*, 234–242.
- Wu, S., Peng, S., Zhang, X., Wu, D., Luo, W., Zhang, T., Zhou, S., Yang, G., Wan, H., & Wu, L. (2015). Levels and health risk assessments of heavy metals in urban soils in Dongguan, China. *Journal of Geochemical Exploration*, *148*, 71–78.
- Wu, Y.-G., Xu, Y.-N., Zhang, J.-H., & Hu, S.-H. (2010). Evaluation of ecological risk and primary empirical research on heavy metals in polluted soil over Xiaoqinling gold mining region, Shaanxi, China. *Transactions of Nonferrous Metals Society of China*, *20*, 688–694.
- Zheng, S., Wang, Q., Yuan, Y., & Sun, W. (2020). Human health risk assessment of heavy metals in soil and food crops in the Pearl River Delta urban agglomeration of China. *Food Chemistry*, *316*, 126213.

**Publisher's Note** Springer Nature remains neutral with regard to jurisdictional claims in published maps and institutional affiliations.